Effect of process parameters on RF magnetron sputtered hydrogenated amorphous silicon thin films

SUTAPA BADYAKAR[1], G. MOHAN RAO[2], CHANDASREE DAS[1,*]
Department of Electrical and Electronics Engineering, BMS College of Engineering, Bangalore, India
Research Cell, RGUKT (AP-IIIT), Nuzvid, India

Characteristics of a-Si:H films deposited by RF magnetron sputtering is investigated in relation to variation in deposition parameter. The deposition rate reduces with substrate bias and hydrogen content, but increases with higher power and temperature. The hydrogen content rises with increased power, bias, and hydrogen flow, but falls with higher temperature. The bandgap widens with bias and hydrogen content but narrows with power and temperature. The hydrogen content can vary from 1.57 at.% to 10.3 at.%, and the bandgap can be changed from 1.2 eV to 1.7 eV. Despite being porous, thin films formed at high temperature shows higher order.

1. Introduction

In order to use hydrogenated amorphous silicon (a-Si:H) thin films as the active layer in photovoltaic cells [1, 2], hydrogen plays a pivotal role in the passivation process [3]. Several methods, including hot-wire chemical vapour deposition (HWCVD) [4], sputtering [5], plasma enhanced chemical vapour deposition (PECVD) [6], and chemical vapour deposition (CVD) [7] are used to assemblage a-Si:H thin films. The majority of high-quality films are made using various CVD techniques, although these techniques are not economical [8], while PVD techniques like RF magnetron sputtering are inexpensive and have better deposition parameter control [9]. Sputtering is a preferred method due to its upraised directed agglomeration and low operation temperature and results in dense coatings with excellent adhesion [10]. The applied RF power, substrate bias, hydrogen dilution in the chamber and the temperature of the substrate are crucial variables in managing the Si network. Up to a certain point, increasing RF power is advantageous, but above that point, very intense ionic bombardment damages the film's surface [11]. Although it needs deeper understanding, there should be a strong connection between the properties of the deposited material and the amount of hydrogen present in the deposition chamber.

This study focuses on hydrogenated amorphous silicon thin films prepared by RF sputtering at varied RF generating power, at various substrate bias, at various hydrogen partial pressures and at various deposition temperatures. The deposited films are examined using optical profiler, UV visible spectroscopy, scanning electron microscopy (SEM) and Fourier Transform Infrared (FTIR) spectroscopy methods with the goal of determining the impact of hydrogen on their nature and characteristics.

2. Experimental

An argon and hydrogen mixed plasma is used to sputter silicon target with 2-inch diameter and 6 mm thickness. Soda lime glass and n-type Si wafers with <100> orientation and 1-10 ohm-cm resistivity are used as substrates. Glass substrates are ultrasonically cleaned in acetone for 15 minutes, cleansed in de-ionized water and then air dried. Silicon wafers are cleaned ultrasonically in acetone for 15 minutes, dipped in 10 % diluted hydrofluoric acid followed by deionized water rinse. A starting chamber pressure of 4.8×10^{-6} mbar and a throw distance of 6 cm are maintained in the chamber. 10 minutes of pre-sputtering is carried out before all the depositions. All samples are deposited for 2 hours and 30 minutes with a constant flow of 23 sccm of argon and at a working pressure of 5×10^{-3} mbar. Each experiment consists of four sets; with the variations in the RF power, concentration of hydrogen flow in the chamber, substrate bias, and substrate temperature, keeping all other parameters constant. As shown in Table 1, each set of experiments has a different set of deposition parameters. The initial experiments are carried out at room temperature (RT), maintaining negative substrate bias voltage at 100 V and hydrogen in-flow at 5 sccm and varying RF power from 50 W to 70 W with a step of 10 Watt. In the second set of experiments, negative substrate bias is changed from 50 V to 150 V, with a step of 50 V while keeping RF power and hydrogen flow at 70 W and 5 sccm, respectively. Third set of trial consists of variation of hydrogen flow from 5 sccm, to 10 sccm with a step of 2.5 sccm carried out at room temperature keeping RF power and negative substrate bias constant at 70 W and 100V respectively. The final set of trials are carried out by varying the deposition temperature from 150 °C to 200 °C and then to 250 °C maintaining RF power at 70 W,

negative substrate bias at 100 V, and hydrogen flow at 5 sccm. The Taylor Hobson-TalySurf CCI optical profilometer is used to measure the growth of the deposited films on the Si wafer. On a Perkin Elmer-Frontier MIR instrument, the basic vibrational modes are found using FTIR spectroscopy. Further the absorption data are obtained from an HR4000CG-UV-NIR Spectrometer, and bandgap calculations are carried out using Tauc Plot [12]. For morphological studies SEM images are obtained from TESCAN-VEGA3 LMU instrument.

Table 1. Deposition parameters variation

Parameter	Quantity variation				Quantity constant			
					RF power (watt)	Substrate bias (volts)	Hydrogen flow (sccm)	Temperature (°C)
RF Power (watt)	50	60	70	-	100	5	RT	
Substrate Bias (volts)	50	100	150	70	-	5	RT	
Hydrogen flow (sccm)	5	7.5	10	70	100	-	RT	
Temperature (°C)	150	200	250	70	100	5	-	

3. Results

The thickness of the a-Si:H thin films is measured using an optical profiler. The thickness and the deposition time are used to compute the deposition rate. Fig. 1a-d display the variation of deposition rate with variations in RF power, substrate bias, hydrogen flow and substrate temperature respectively.
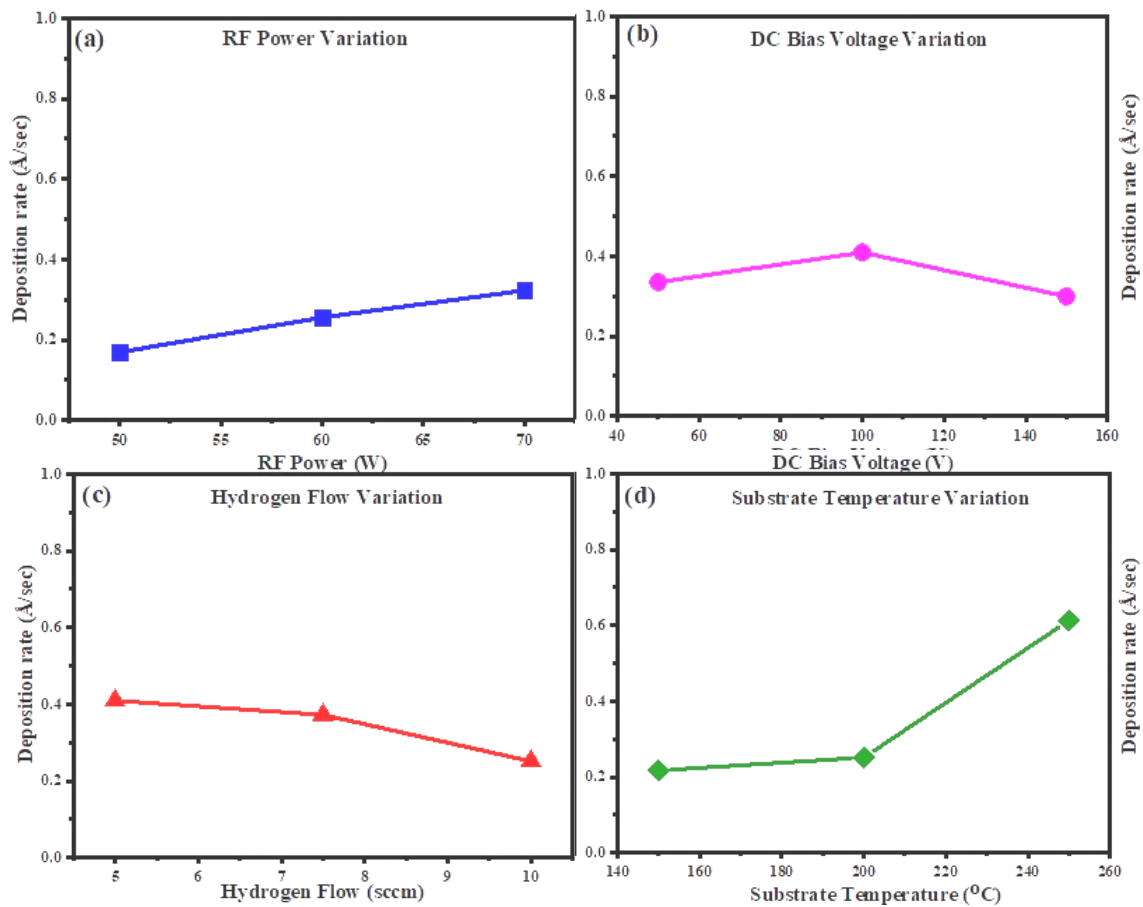

Fig. 1. Plots for deposition parameter variation (a) RF power; (b) DC bias voltage (c) hydrogen flow (d) Substrate temperature Vs deposition rate (color online)

The FTIR absorption spectra with variations of RF power, substrate bias, and hydrogen flow and substrate temperature are shown in Fig. 2a-d respectively. The stretching vibration modes have been found to be well-located between 2000 cm^{-1} and 2100 cm^{-1} as shown in Table 2. It indicates that when hydrogen gas is added to

the vacuum container along with the argon gas while sputtering a silicon target, a Si-H bond is formed [13]. Calculations are done using a widely used area approximation method for infrared absorption bands which indicate the concentration of bonded hydrogen [14]. Integrating the region under the absorption band and following the steps outlined in a prior study, the hydrogen content (C_H) of the films is determined [15]. The expression below provides it:

$$C_H = [(A_\omega \int \alpha(\omega)d\omega/\omega)/ N_{si}] \times 100\%$$

where $A_\omega = 1.6 \times 10^{19}$ cm^{-2}, $N_{si} = 5 \times 10^{22}$ cm^{-3}, $\alpha(\omega)$ is the absorption coefficient and ω is the Wavenumber in cm^{-1}.

The relationship between variation in RF power, hydrogen flow, substrate bias and substrate temperature with rate of deposition and bandgap is also presented in Table 2. The bandgap of the films is calculated using the Tauc and Davis-Mott relation [12],

$$(\alpha h\upsilon)^{1/n} = k (h\upsilon - E_g)$$

where $\alpha = (1/d) \times \ln (1/A)$ and $h\upsilon = h (c/\lambda)$.

Further α is the absorption coefficient, d is the thickness of the thin film, A is the absorbance, h is the Planck's constant, c is speed of light, υ is the frequency of the incident photon, $h\upsilon$ is incident photon energy, λ is the wavelength, n is the nature of transition of the material, k is the constant and E_g is the bandgap energy.
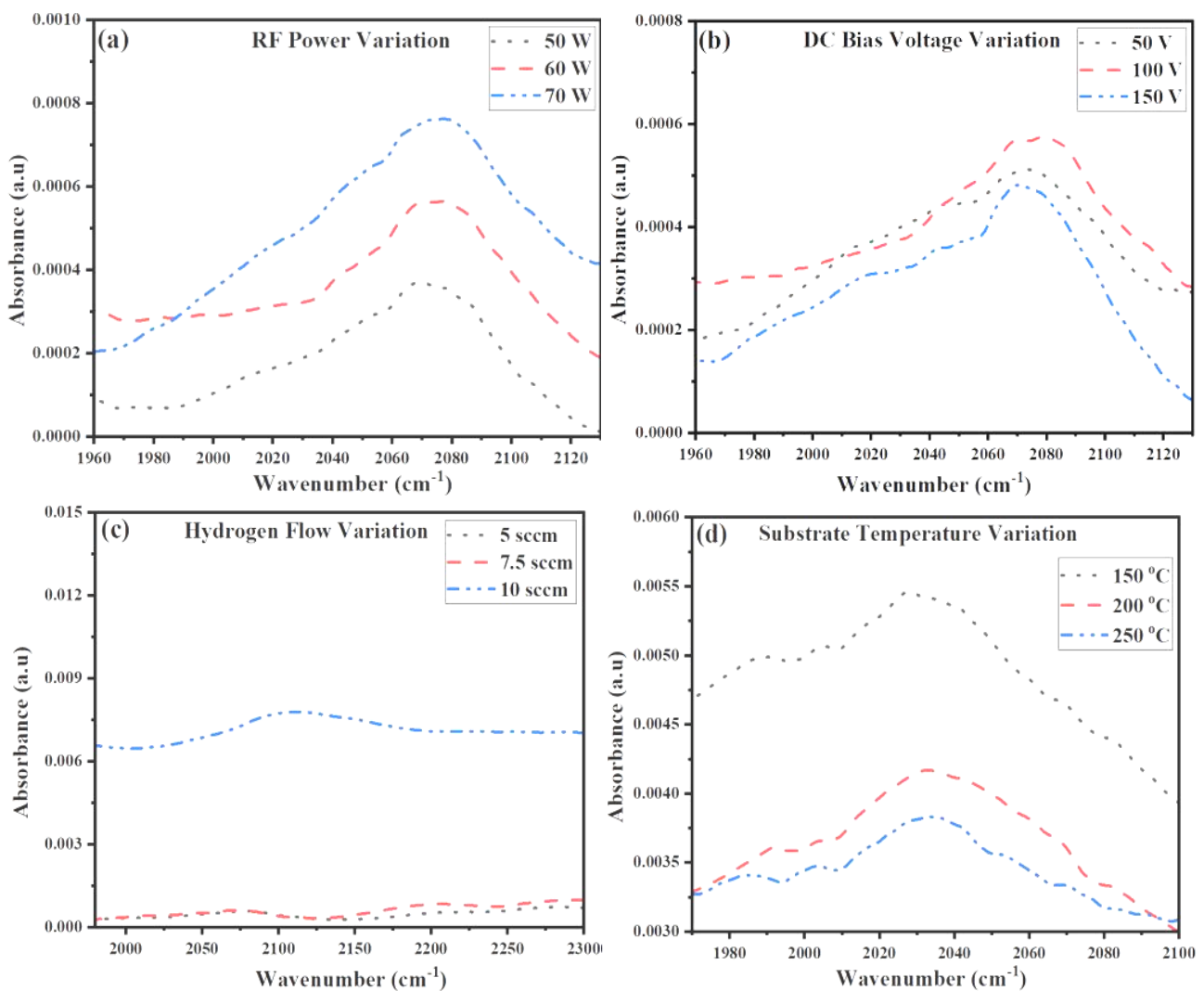

Fig. 2. FTIR plots for deposition parameter variation (a) RF power; (b) DC bias voltage; (c) hydrogen flow; (d) substrate temperature, wavenumber vs absorbance (color online)

The hydrogen content and optical bandgap of a film can vary across a wide range depending on the deposition parameters [16]. The hydrogen concentration in an a-Si:H thin film solar-cell is crucial because it is headlong related to many of the special characteristics of the material that are absent in discharged a-Si thin films [17,18]. It is believed that 10-20 at.% presence of hydrogen in the films

results in better quality solar cells [19]. When silicon is ejected in the presence of hydrogen, the hydrogen is known to bond to the silicon in the form of a-Si:H. It is observed that while the rate of deposition of silicon atom accelerates the amount of hydrogen atoms in the films declines. Fig. 3a-d display the plots for the changes in hydrogen content in each film due to changes in RF

power, substrate bias, hydrogen flow and substrate temperature respectively. The optical band gap in the deposited films ranged from 1.2 eV to 1.7 eV and is in conformity with literature [20,21]. The variation in bandgap due to change in RF power, substrate bias, hydrogen flow and substrate temperature are shown in Fig. 4 (a-d) sequentially. The optical bandgap range suggests that a-Si is bonded with hydrogen [21].

For morphological studies, four samples are selected from Table 1, which are renamed in Table 3 as sample 1-4. Sample1 has been chosen as the base sample (Fig. 5a). It is prepared by depositing hydrogenated amorphous silicon on glass at ambient temperature using a 70 W RF power

source, a negative substrate bias of 100 V, and a hydrogen flow of 5 sccm. Keeping this sample as the base for remaining three samples, only one parameter out of substrate bias (Fig. 5b), hydrogen flow (Fig. 5c), and deposition temperature (Fig. 5d) is varied while keeping others identical. With a bandgap value of 1.2 eV for sample 2, the grains are found to be less clubbed, and with a bandgap value of 1.5 eV for sample 3, structures are flaky in nature. In sample 4, the bandgap is 1.25 eV and the grains are dense and slightly organized. The base sample1 displays a porous surface picture with a bandgap of 1.47 eV.
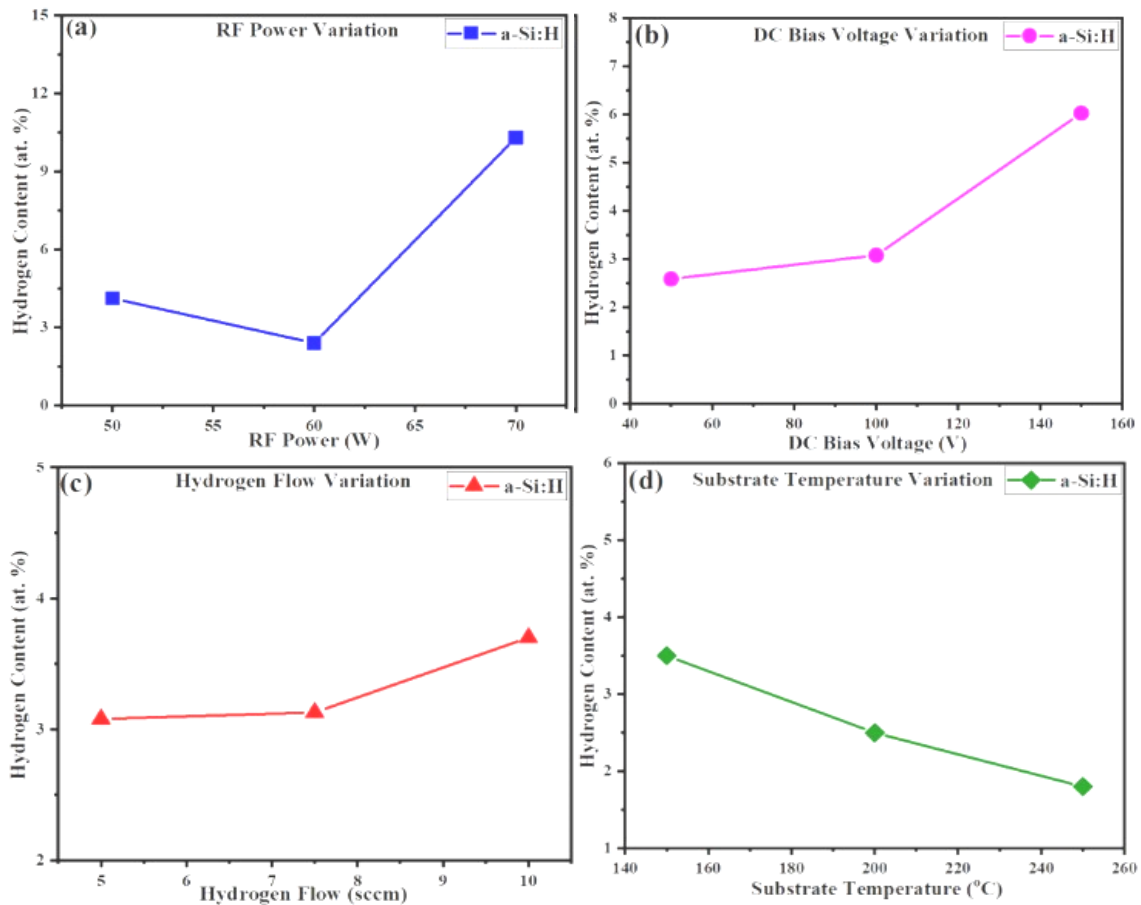

Fig. 3. Plots for deposition parameter variation (a) RF power; (b) DC bias voltage (c) hydrogen flow (d) Substrate temperature vs hydrogen content variation (color online)

Table 2. Peak value of wavenumber, deposition rate and bandgap with deposition parameters variation

Deposition Parameter		Peak value of wavenumber (cm^{-1})	Deposition rate (Å/sec)	Bandgap (eV)
RF Power (watt)	50	2069	0.169	1.43
	60	2077	0.256	1.41
	70	2078	0.323	1.39
Substrate Bias (volts)	50	2045	0.335	1.2
	100	2079	0.409	1.42
	150	2071	0.299	1.55
Hydrogen flow (sccm)	5	2079	0.409	1.47
	7.5	2070	0.372	1.50
	10	2100	0.251	1.70
Temperature (°C)	150	2028	0.217	1.27
	200	2033	0.251	1.41
	250	2035	0.613	1.25

Table 3. Deposition parameters variation for SEM along with bandgap

Parameter and sample name	Quantity Constant				Bandgap (eV)
	RF power (watt)	Substrate bias (volts)	Hydrogen flow (sccm)	Temperature (°C)	
(a)Sample 1	70	100	5	RT	1.47
(b)Sample 2	70	50	5	RT	1.2
(c)Sample 3	70	100	7.5	RT	1.5
(d)Sample 4	70	100	5	250	1.25

4. Discussion

4.1. Effect of RF power variation

It has been found that rising the RF power from 50 W to 60 W and then to 70 W causes a modest increase in the build-up rate for the films as shown in Fig. 1a. The rise in the film thickness is approximately linear as RF power increases. The segregation and ionization of SiH_4 radicals are often accelerated by a rise in RF power, leading to a growth in the flow of the precursor that deposit on the surface of the substrate. This probably has aided in raising the rate of deposition [22, 23].

FTIR plot in Fig. 2a shows that the absorbance value is increasing as the RF power is escalated gradually from 50 W to 70 W. According to the findings, the hydrogen concentration is initially 2.5 at.% in case of films sputtered at 50 W power and increases to 4.12 at.% when power is increased to 60 W. Increase in concentration to 10.3 at.% with escalated RF power of 70 W, has shown the highest rate of deposition with more hydrogen incorporation into the film. The related plot is shown in Fig. 3a.

The bandgap gradually declines from 1.43 eV to 1.39 eV when RF power is advanced from 50 W to 70 W confirming a linear decline with increase in RF power. The Tauc plot represented in Fig. 4a shows a photon energy decline as the RF power is increased.
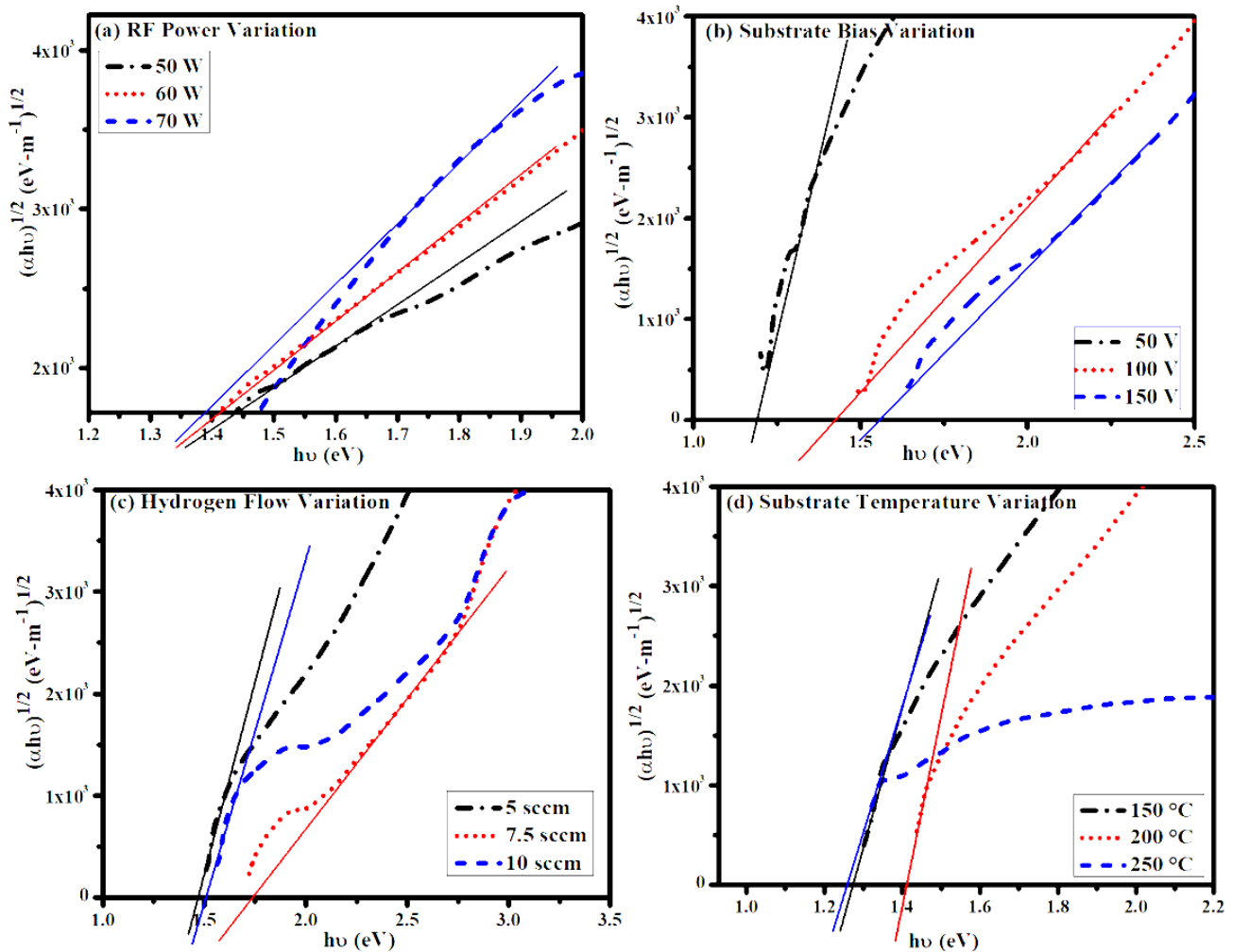

Fig. 4. Tauc plots for deposition parameter variation (a) RF power; (b) substrate bias; (c) hydrogen flow; (d) substrate temperature, where bandgap is determined (color online)

4.2. Effect of substrate bias variation

When a negative DC voltage is given to the substrate, the rate increases from 50 V to 100 V initially but decreases thereafter till 150 V as shown in Fig. 1b. Surface charges will be positive on a negatively biased substrate, which will cause a local shift in the plasma. Additionally, this charge impact reduces the plasma substrate potential and, therefore, the ion stream [24]. So, a difference in the growth rate is evident.

Fig. 2b depicts that the absorbance is highest with a substrate bias of 100 V. When the negative substrate bias is raised from 50 V to 150 V, the hydrogen concentration in the thin films steadily increases from 2.59 at.% to 6.03 at.%. However, the deposition rate initially increases when bias is between 50 and 100 V, thereafter declines till 150 V depicted in Fig. 3b. The reason could be the high negative bias applied to the substrate, which may cause re-sputtering of atoms, resulting in decrease in deposition rate [25].

The bandgap rapidly increases, from 1.2 eV to 1.42 eV and then to 1.55 eV along with an increase in the hydrogen concentration in the films, as the substrate bias is raised linearly from 50 V to 100 V and then to 150 V respectively. The Tauc plot is shown in Fig. 4b where the energy bandgap shown for 100 V substrate bias is 1.42 eV which is suitable for an absorber layer material for photovoltaic application.

4.3. Effect of hydrogen concentration variation

When the hydrogen concentration is increased keeping the flow of argon constant during the deposition, the deposition rate decreases steadily as shown in Fig. 1c. Sputtering environment becomes diluted after hydrogen insertion in the argon atmosphere. Since hydrogen atoms are lighter than argon, they effectively dilute the pure argon plasma, which has the highest momentum transfer. Variations in the deposition rate are also caused due to the reactions in the plasma [26]. These could be the reasons for a lower rate of deposition and hence less transfer of material.

FTIR plot shown in Fig. 2c suggests that absorbance is maximum for 10 sccm of hydrogen flow. The hydrogen concentration in the films steadily increases from 3.08 at.% to 3.7 at.% as the hydrogen flow is gradually raised from 5 sccm to 10 sccm as shown in Fig. 3c. When the hydrogen concentration in the chamber is higher, the deposition rate is slower, resulting in lower deposition of silicon atoms.

When the hydrogen flow is escalated from 5 sccm to 7.5 sccm, the bandgap increases from 1.47 eV to 1.5 eV initially and then rapidly to 1.7 eV at 10 sccm of hydrogen. Tauc plot shown in Fig. 4c suggests that the bandgap of 1.47 eV at 5 sccm could be applicable for an absorber layer material.

4.4. Effect of substrate temperature variation

With the escalation in the deposition temperature from 150 °C to 200 °C, the rate of deposition rises gently and thereafter increases rapidly at 250 °C, keeping RF power, substrate bias and hydrogen flow constant as shown in Fig. 1d. When temperature rises, the formation of a-Si:H will be accelerated initially but later hydrogen atoms escape from the expanded surface [11].

Fig. 2d shows that the absorbance is highest for 150°C substrate temperature. As the deposition temperature rises from 150°C to 200°C, the hydrogen concentration declines gradually from 3.5 at.% to 2.5 at.% and with further increase in temperature to 250°C the concentration of hydrogen dips to 1.57 at.%. This trend is shown in Fig. 3d.

There is a steady rise in bandgap from 1.27 eV to 1.41 eV with temperature from 150 °C to 200 °C respectively. Thereafter a significant dip to 1.25 eV is evident at 250°C as shown in Fig. 4d. With rise in temperature, the concentration of hydrogen in the film decreases, contributing to the decrease in bandgap [27]. In contrast to the films sputtered at 150°C and 250°C, film sputtered at 200°C shows a higher bandgap value. This could be due to higher degree of consistency in grain shape and size, and a lower defect density towards the edges of the band for the film coated at 200 °C [28].

4.5. Surface morphology

Fig. 5a-d display SEM images at various deposition conditions as shown in Table 3 for four different samples. Sample1 is kept as the base sample (Fig. 5a) and compared by other three (Fig. 5b-c) as one parameter is varied. When the bias voltage is reduced, the image (Fig. 5b) demonstrates that the grains are less clubbed than in the first image (Fig. 5a). The surface picture takes a clogged appearance as hydrogen flow is increased (Fig. 5c). According to the reported studies, hydrogenation deteriorates the crystallinity of the thin film [29,30]. The grains are slightly structured and dense when heating is deployed to the substrate (Fig. 5d). The surface morphology of a-Si:H thin films is clearly seen in these photos. It is explicit from the sample's surface that they are made of porous amorphous silicon and hardly dense. When the particles are clubbed, they are about 200 nm in size and have a porosity of 100 nm (Fig. 5d). According to bandgap values in Table 3, as hydrogen flow is decreased, bandgap decreases and more clear grains become apparent. Further as the substrate bias is decreased, bandgap increases, and with the addition of temperature, bandgap further declines and the distance between the grain dips. The reduced porosity, improvement in the density has an effect on the bandgap and it reduces drastically as seen in Fig 2d.
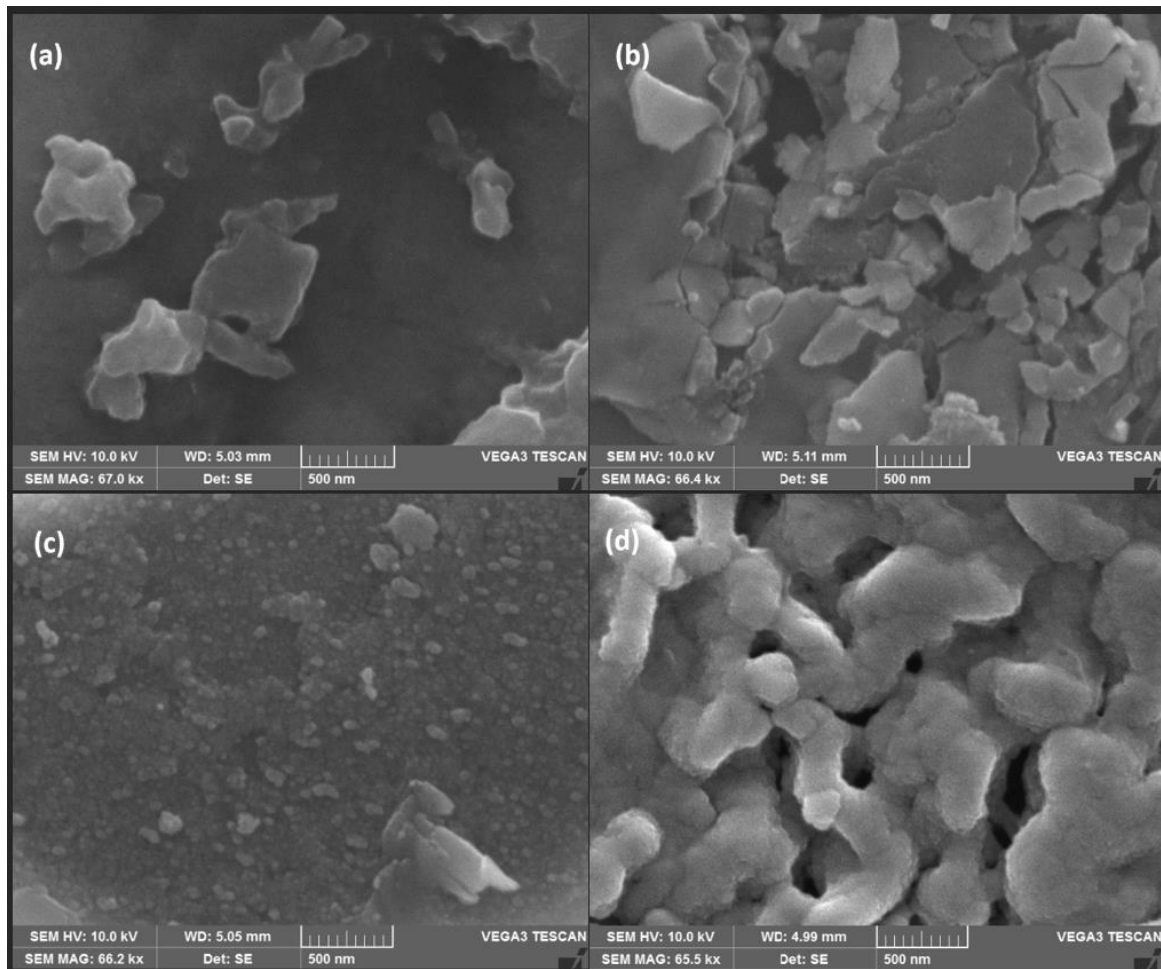
Fig. 5. SEM images of a-Si:H thin films shows the porous nature of each sample (a) sample1 (b) sample2 (c) sample3 (d) sample4

5. Conclusions

The variation of the deposition rate in relation to the alteration of the experimentation settings is carried out. Further, FTIR is used to determine the concentration of hydrogen incorporation in the films. It is observed that a drop in the deposition rate with increased hydrogen concentration is a sign of more significant selective etching caused by a rise in silicon hydride radical concentration. Hydrogen has been incorporated in the thin films by various ways, like changing the RF power, changing the substrate bias, changing the hydrogen in-flow and finally changing the deposition temperature. Dilution of hydrogen also significantly slows down the pace of deposition. Poor deposition rate is a significant impediment to its efficient use. Defects are present in the grain boundaries, as can be seen in SEM images, which may impact the properties. When substrate bias and substrate temperature are increased to 100 volts and 250 °C, the band gap value is very low due to reduction in porosity, onset of crystallinity and reduced hydrogen content in the films. A detailed study on the effect of structural changes on the behavior of a-Si:H films is being done. All the films are amorphous in nature but the growth structures need to be controlled to get a good a-Si:H thin film where the hydrogen helps in passivating the defects.

References

[1] S. Badyakar, C. Das, Mater. Today Proc. **62**(8), 5275 (2022).
[2] S. Badyakar, C. Das, J. of Jilin Univ. **41**(10), 229 (2022).
[3] H. Shaik, V. Anand, M. Rao G, Mater. Sci. Semicond. Process **26**, 367 (2014)
[4] S. R. Jadkar, J. V. Sali, M. G. Takwale, D. V. Musale, S. T. Kshirsagar, Sol. Energy Mater. Sol. Cells **64**(4), 333 (2000).
[5] X. Wang, S. Wang, D. Zhu, X. Huang, J. Optoelectron. Adv. M. **25**(11-12), 594 (2023).

[6] S. C. Saha, S. Ghosh, S. Ray, Sol. Energy Mater. Sol. Cells **45**(2), 115 (1997).

[7] A. Masuda, Y. Ishibashi, K. Uchida, K. Kamesaki, A. Izumi, H. Matsumura, Sol. Energy Mater. Sol. Cells **74**(1-4), 373 (2002).

[8] M. Hossain, H. H. Abu-Safe, H. Naseem, W. D. Brown, J. Non Cryst. Solids **352**(1), 18 (2006).

[9] A. Achiq, R. Rizk, F. Gourbilleau, P. Voivenel, Thin Solid Films **348**(1-2), 74 (1999).

[10] Y. Sheng, J. Qiao, Z. Zhang, J. Optoelectron. Adv. M. **23**(11-12), 574 (2021).

[11] M. Jana, D. Das, A.K. Barua, Journal of Applied Physics **91**(8), 5442 (2002).

[12] J. Tauc, Amorphous and liquid semiconductors, Springer, Boston, MA, 159 (1974).

[13] F. Finger, V. Viret, A. Shah, X-M. Tang, J. Weber, W. Beyer, MRS Online Proceedings Library **192**, 583 (1990).

[14] A. H. Mahan, L. M. Gedvilas, J. D. Webb, Journal of Applied Physics **87**, 1650 (2000).

[15] F. Z. Sahraoui, A. Kebab, A. Bouhekka, J. D. Sib, Y. Bouizem, D. Benlakehal, L. Chahed, Optik **168**, 65 (2018).

[16] P. Koidl, C. Wild, B. Dischler, J. Wagner, M. Ramsteiner, Materials Science Forum, Trans. Tech. Publications Ltd. **52-53**, 41 (1990).

[17] J. Shao, X. Xi, G. Liu, F. Luo, J. Optoelectron. Adv. M. **25**(5-6), 228 (2023).

[18] A. A. Dakhel, J. Optoelectron. Adv. M. **24**(1-2), 35 (2022).

[19] P. J. Zanzucchi, C. R. Wronski, D. E. Carlson, Journal of Applied Physics **48**(12), 5227 (1977).

[20] S. Knief, W. von Niessen, Physical Review B **59**(20), 12940 (1999).

[21] W. E. Carlos, P. C. Taylor, Physical Review B **25**, 1435 (1982).

[22] A. Chowdhury, S. Mukhopadhyay, S. Ray, Solar Energy Materials and Solar Cells **92**(4), 385 (2008).

[23] S. Lebib, P. Roca i Cabarrocas, J. Applied Physics **97**, 104334 (2005).

[24] F. Alvarez, P. Prieto, A. Florez, L. Tirado, L.F. Castro, Journal of Applied Physics **65**(12), 4869 (1989).

[25] T. I. Selinder, G. Larsson, U. Helmersson, S. Rudner, Journal of Applied Physics **69**(1), 390 (1991).

[26] W. A. Lanford, M. J. Randm, Journal of Applied Physics **49**(4), 2473 (1978).

[27] J. Shirafuji, M. Kuwagaki, T. A. Sato, Y. Inuishi, Japanese Journal of Applied Physics **23**(10R), 1278 (1984).

[28] P. Chelvanathan, Y. Yusoff, F. Haque, M. Akhtaruzzaman, M. M. Alam, Z. A. Alothman, M. J. Rashid, K. Sopian, N. Amin, Applied Surface Science **334**, 138 (2015).

[29] M. J. Eshraghi, M. Bordbari, N. Naderi, A. S. A. Hosseinzadeh, J. Optoelectron. Adv. M. **25**(9-10), 494 (2023).

[30] P. Datta, M. Sharmin, J. Podder, S. Choudhury, J. Optoelectron. Adv. M. **25**(9-10), 508 (2023).

_____

*Corresponding author: chandasreedas.eee@bmsce.ac.in